

Distinct potassium channel types in brain capillary pericytes

Maria Sancho,^{1,2,*} Nicholas R. Klug,¹ Osama F. Harraz,^{1,3} David Hill-Eubanks,¹ and Mark T. Nelson^{1,3,4,*}

¹Department of Pharmacology, University of Vermont, Burlington, Vermont; ²Department of Physiology, Faculty of Medicine, Complutense University of Madrid, Madrid, Spain; ³Vermont Center for Cardiovascular and Brain Health, Larner College of Medicine, University of Vermont, Burlington, Vermont; and ⁴Division of Cardiovascular Sciences, University of Manchester, Manchester, United Kingdom

ABSTRACT Capillaries, composed of electrically coupled endothelial cells and overlying pericytes, constitute the vast majority of blood vessels in the brain. The most arteriole-proximate three to four branches of the capillary bed are covered by α -actin-expressing, contractile pericytes. These mural cells have a distinctive morphology and express different markers compared with their smooth muscle cell (SMC) cousins but share similar excitation-coupling contraction machinery. Despite this similarity, pericytes are considerably more depolarized than SMCs at low intravascular pressures. We have recently shown that pericytes, such as SMCs, possess functional voltage-dependent Ca^{2+} channels and ATP-sensitive K^{+} channels. Here, we further investigate the complement of pericyte ion channels, focusing on members of the K^{+} channel superfamily. Using NG2-DsRed-transgenic mice and diverse configurations of the patch-clamp technique, we demonstrate that pericytes display robust inward-rectifier K^{+} currents that are primarily mediated by the Kir2 family, based on their unique biophysical characteristics and sensitivity to micromolar concentrations of Ba^{2+} . Moreover, multiple lines of evidence, including characteristic kinetics, sensitivity to specific blockers, biophysical attributes, and distinctive single-channel properties, established the functional expression of two voltage-dependent K^{+} channels: K_v1 and BK_{Ca} . Although these three types of channels are also present in SMCs, they exhibit distinctive current density and kinetics profiles in pericytes. Collectively, these findings underscore differences in the operation of shared molecular features between pericytes and SMCs and highlight the potential contribution of these three K^{+} ion channels in setting pericyte membrane potential, modulating capillary hemodynamics, and regulating cerebral blood flow.

SIGNIFICANCE The physiological role of capillary pericytes in regulating cerebral blood flow (CBF) remains obscure, largely owing to an incomplete understanding of the electrophysiological properties of these cells. In this study, we take a further step toward building a comprehensive electrophysiological framework of native brain capillary pericytes, elucidating their K^{+} channel repertoire as well as differences in the electrophysiological signature of these cells compared with that of smooth muscle cells. The insights gained through this analysis are essential for deciphering the complete biophysical profile and influence of pericytes on capillary blood flow. Pericyte signaling mechanisms involving K^{+} channels, including their role in V_M and the regulation of CBF, represent an exciting avenue for future exploration in both physiological and pathological contexts.

INTRODUCTION

The brain cerebral vasculature is composed of surface (pial) arteries that further divide into progressively smaller penetrating (parenchymal) arterioles. Arteries and arterioles consist of an inner lining of endothelial cells (ECs) wrapped by a single (arterioles) or multiple (arteries) concentric layers of contractile smooth muscle cells (SMCs). As these arterioles penetrate deeper into the brain, they branch to

form a vast network of capillaries that massively extends the territory of blood perfusion, effectively covering all regions of the brain (1). This brain angioarchitecture strategically positions capillaries in intimate association with all neurons, enabling efficient exchange of nutrients and waste products (2). Unlike arteries and arterioles, capillaries lack an SMC layer, instead consisting of continuous tubes formed by tight-junction-connected capillary ECs (cECs) that are discontinuously overlain by pericytes, with which they share a common basement membrane.

In brain surface arteries and penetrating arterioles, the membrane potential (V_M) of SMCs plays a central role

Submitted November 15, 2023, and accepted for publication March 1, 2024.

*Correspondence: masanc75@ucm.es or mark.nelson@uvm.edu

Editor: Valeria Vasquez.

<https://doi.org/10.1016/j.bpj.2024.03.004>

© 2024 Biophysical Society.

Sancho et al.

in pressure-induced constriction (myogenic tone) (3). This myogenic response is a major component of the autoregulation process, which is essential for maintaining relatively constant cerebral blood flow (CBF) in the face of fluctuations in blood pressure and thereby protects the brain microvasculature against damaging surges in pressure and ensures adequate basal tissue perfusion. Notably, pericytes have also been shown to play a crucial role in regulating capillary diameter to control blood flow (4).

SMCs in penetrating arterioles, such as those in surface pial arteries, exhibit a V_M of approximately -60 mV at low intravascular pressure (20 mm Hg) and depolarize to about -40 mV at physiological pressures (40 mmHg) (3,5). This depolarization activates voltage-dependent Ca^{2+} channels (VDCCs), leading to increased Ca^{2+} entry, elevation of intracellular Ca^{2+} , and subsequent Ca^{2+} -dependent arteriolar constriction (the sequence of events underpinning the myogenic response (3)). The V_M of SMCs in pressurized cerebral arteries (approximately -40 mV) is controlled by the concerted interplay of potassium (K^+) channels, including voltage-dependent (K_V), large-conductance Ca^{2+} -activated (BK_{Ca}), inwardly rectifying (Kir2.1), and ATP-sensitive (K_{ATP}) K^+ channels (6). The K^+ equilibrium potential (E_K) for cerebral artery SMCs is about -100 mV at a physiological extracellular K^+ concentration (~ 3 mM). The opening of K^+ channels increases K^+ efflux, leading to V_M hyperpolarization, which in turn reduces the activity of VDCCs, causing a decrease in intracellular Ca^{2+} and thus vasodilation (6,7).

In sharp contrast to the case in SMCs, capillary pericytes are relatively depolarized at low pressures (-40 vs. -60 mV) but unlike SMCs are not constricted at this V_M (8); they do, however, further depolarize and constrict in response to higher pressures. RNA sequencing data suggest that pericytes express diverse K^+ channels (9) that could be involved in dynamically modulating the V_M of these cells in response to vasoactive agents and/or neural activity. However, direct measurements of the activity of ion channels and characterization of their molecular attributes in native brain pericytes are largely lacking, representing a major gap in our understanding of how this cell type contributes to vascular regulation. Our recent studies have begun to define the repertoire of ion channels expressed in the membrane of central nervous system (CNS) pericytes and to elucidate their impact on capillary V_M and CBF (8,10). In this context, we recently demonstrated that pericytes possess functional K_{ATP} channels, which are activated indirectly by vasoactive mediators, such as adenosine and calcitonin-gene-related peptide, which signal via the adenylyl cyclase/cyclic AMP/protein kinase A pathway to profoundly hyperpolarize resting V_M and increase CBF (10). We have further found that CNS capillary pericytes are equipped with VDCCs, which appear to variably affect pericyte Ca^{2+} signals depending on the loca-

tion of the pericyte along the arteriole proximate-to-distal continuum (8).

Here, we demonstrate the functional expression of three distinct K^+ channel types in single pericytes from brain capillaries. Native pericytes were obtained by mechanical disruption and enzymatic dissociation of NG2-DsRed transgenic mouse brains and identified based on specific morphological criteria, NG2 expression, and NeuroTrace labeling. K^+ channels were studied using the conventional or perforated whole-cell configuration or cell-attached mode of the patch-clamp technique. Notably, pericytes exhibited a robust inward current that was sensitive to micromolar concentrations of barium (Ba^{2+}), a hallmark of strongly inwardly rectifying K^+ (Kir2) channels. We further observed two voltage-dependent outward currents. The first was identified as a K_V1 channel current based on its characteristic kinetics and sensitivity to 4-aminopyridine (4-AP). The second was determined to be a BK_{Ca} channel current based on multiple lines of evidence: 1) its sensitivity to the specific blockers, paxilline and iberiotoxin; 2) its role in generating ryanodine-sensitive, spontaneous transient outward currents (STOCs), which are known to be mediated by BK_{Ca} channels; and 3) its characteristic single-ion channel conductance properties. These findings are significant as these three ion channel families may have profound impacts on the regulation of pericyte resting V_M and capillary blood perfusion.

MATERIAL AND METHODS

Animal procedures

Adult (2- to 3-month-old) male NG2-DsRed mice, obtained from Jackson Laboratories (USA), were housed on a 12-h light/dark cycle with environmental enrichment and unrestricted access to food and water. For experimental procedures, mice were euthanized by intraperitoneal injection of sodium pentobarbital (100 mg/kg) and rapidly decapitated. All animals were used in strict accordance with the guidelines and protocols approved by the Institutional Animal Care and Use Committee of the University of Vermont.

Chemicals

Iberiotoxin and 4-AP were purchased from Tocris Bioscience (USA); paxilline was obtained from Cayman Chemical Company (USA); and ryanodine was acquired from Enzo Life Sciences (USA). Unless stated otherwise, all other chemicals utilized in the study were obtained from Sigma-Aldrich (USA).

Isolation and identification of native pericytes

Single capillary pericytes were isolated from NG2-DsRed mouse brains by mechanical dissociation (Fig. 1) using a papain-based neural tissue dissociation kit (Miltenyi Biotec, USA) as previously described (10,11). Briefly, a small piece of somatosensory cortex (~ 10 – 20 mm³) was carefully dissected and minced into small fragments using sharp scissors. The brain tissue fragments were transferred to isolation solution composed of 55 mM NaCl, 80 mM Na-glutamate, 5.6 mM KCl, 2 mM MgCl₂,

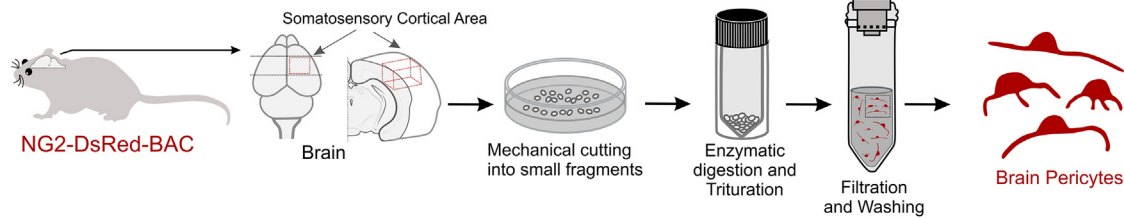


FIGURE 1 Experimental approach for isolating native pericytes from brain capillaries for use in patch-clamp electrophysiology. Pericytes were isolated from NG2-DsRed-BAC transgenic mouse brains by mechanical disruption and enzymatic dissociation. A small portion of the somatosensory cortex of the mouse brain was dissected and cut into small fragments using sharp scissors. The tissue fragments were then transferred to isolation solution and exposed to a two-step digestion process consisting of a 17-min incubation in isolation solution containing enzyme 1 (37°C) followed by a 12-min incubation with enzyme 2. The brain suspension was then triturated to yield single cells and incubated for an additional 12 min at 37°C. The cell suspension was filtered through a 62- μm nylon mesh and diluted by adding 3 mL of cold isolation solution. The resulting single brain capillary pericytes, identified by their DsRed fluorescence, were then ready for patch-clamp analyses.

4 mM glucose, and 10 mM HEPES (pH 7.3) containing “enzyme 1” (provided in the kit), and incubated for 17 min at 37°C. “Enzyme 2” was then added, and the brain suspension was mixed by gently pipetting up and down (~ 10 times) using a Pasteur pipette. The brain suspension was incubated for an additional 12 min at 37°C, then triturated approximately 10 times using a 20G needle in a 1-mL syringe and incubated for 10 min at 37°C, followed by filtration through a 62- μm nylon mesh to remove debris. After adding 3 mL of cold isolation solution to the filtrate, isolated pericytes were stored in ice-cold isolation solution and used within ~ 5 h of dispersion. At the outset of experiments, pericytes from NG2-DsRed-BAC transgenic mice were first identified by their DsRed fluorescence and characteristic morphology. After patch-clamp experiments, the recorded cell was confirmed as a pericyte based on its positive staining with NeuroTrace 500/525 Green Fluorescent Nissl (1:2000; Thermo Fisher Scientific, USA). The epifluorescence of DsRed and NeuroTrace was recorded with a digital camera attached to the photo port using the respective DsRed and eGFP filter cubes. Separate sets of pericyte and SMC z stack images were acquired using a Revolution dual-camera, spinning-disk confocal microscope system equipped with iXon Life 16-bit EMCCD cameras (Andor Technology) attached to a Nikon microscope. Fluorescence was excited using a 488- or 560-nm laser, and emitted fluorescence was collected through a 527.5/49- or 641.5/117-nm band-pass filter.

Electrophysiology recordings

Patch-clamp electrophysiology was used to measure whole-cell and single-channel currents in native brain pericytes. Currents were amplified using an Axopatch patch-clamp 200B amplifier, filtered at 1 kHz, digitized at 5 kHz, and stored on a computer for offline analysis with Clampfit 10.7 software (Molecular Devices, USA). Patch pipettes were pulled from borosilicate microcapillary tubes (1.5-mm outer diameter and 1.17-mm inner diameter; Sutter Instruments, USA) using a Narishige puller (PC-100; Japan) and fire polished to a tip resistance of 4–5 M Ω . All experiments were performed at room temperature ($\sim 22^\circ\text{C}$). The capacitance of pericytes averaged 10.1 ± 2.1 pF ($n = 62$ pericytes).

Whole-cell currents were recorded in freshly isolated pericytes using either the conventional or perforated whole-cell configuration of the patch-clamp technique. The whole-cell configuration was achieved by gently lowering a micropipette onto a cell and applying negative pressure to create a high-resistance (G Ω) seal and rupture the membrane, allowing access to the interior of the cell. For recording Kir2 currents, cells were voltage clamped at a holding potential of -50 mV and then ramped from -140 to $+40$ mV over 400 ms. The bath solution contained 80 mM NaCl, 60 mM KCl, 1 mM MgCl₂, 10 mM HEPES, 7 mM glucose, and 2 mM CaCl₂ (pH 7.4), and the pipette solution consisted of 10 mM NaOH, 11.4 mM KOH, 128.6 mM KCl, 1.1 mM MgCl₂, 3.2 mM CaCl₂,

5 mM EGTA, and 10 mM HEPES (pH 7.2). For recording K_V currents, the cell bathing solution contained 134 mM NaCl, 6 mM KCl, 1 mM MgCl₂, 10 mM HEPES, 7 mM glucose, and 0.1 mM CaCl₂ (pH 7.4) and the pipette solution consisted of 107 mM KCl, 33 mM KOH, 5 mM NaCl, 2 mM MgCl₂, 10 mM EGTA, 1 mM CaCl₂, and 10 mM HEPES (pH 7.2). For recording BK_{Ca} currents, cells were bathed in an extracellular solution containing 134 mM NaCl, 6 mM KCl, 1 mM MgCl₂, 10 mM HEPES, 7 mM glucose, and 2 mM CaCl₂ (pH 7.4); the composition of the pipette solution was 107 mM KCl, 33 mM KOH, 5 mM NaCl, 1.1 mM MgCl₂, 5 mM EGTA, 3.2 mM CaCl₂, and 10 mM HEPES (~ 300 nM free Ca²⁺; pH 7.2). Whole-cell currents were elicited by 20-mV depolarizing steps (400 ms) from a holding potential of -50 mV to potentials between -70 and $+70$ mV. Whole-cell capacitance and series access resistance were measured using the cancellation circuitry in the voltage-clamp amplifier.

STOCs in isolated pericytes were monitored using perforated patch-clamp electrophysiology. Recording electrodes were backfilled with a pipette solution consisting of 110 mM K-aspartate, 30 mM KCl, 10 mM NaCl, 1 mM MgCl₂, 10 mM HEPES, and 0.05 EGTA (pH 7.2), containing 250 $\mu\text{m}/\text{mL}$ amphotericin B, used to create the perforated configuration. The bath solution composition was 134 mM NaCl, 6 mM KCl, 1 mM MgCl₂, 10 mM HEPES, 10 mM glucose, and 2 mM CaCl₂ (pH 7.4). STOCs were monitored while cells were held at a V_M of -20 mV. The threshold for detection of STOCs was set to about three times the single-channel current of a BK_{Ca} channel, which corresponds to a current amplitude of 10 pA at a V_M of -20 mV.

Single-channel currents were recorded in the cell-attached configuration. To set E_K to 0 mV, we used bath and pipette solutions with a symmetrical composition and included 140 mM KCl, 1.08 mM MgCl₂, 5 mM EGTA, and 3.16 mM CaCl₂ (~ 300 nM free Ca²⁺, pH 7.2). Single-channel activity was monitored while cells were held at a range of V_Ms (from 0 to $+100$ mV in 20-mV increments; applied voltage from 0 to -100 mV); unitary currents were measured, and the slope conductance was subsequently calculated. The average open probability (NP_o) of the channel was calculated directly by dividing the level dwell time by the total time of continuous recording during periods of stable channel activity.

Statistical analysis

Data were analyzed using Clampfit 10.7 software (Molecular Devices, USA) and GraphPad Prism 9 (GraphPad Software). Data are expressed as means \pm standard deviation (SD), with n indicating the number of cells or animals included in the analysis. Where appropriate, paired t -tests were performed to compare the effects of a given treatment. In cases where data were not normally distributed, statistical significance was determined using the Wilcoxon nonparametric test. p values less than 0.05 were considered statistically significant, denoted by stars in figure panels. Sample sizes

Sancho et al.

were estimated based on previous similar experiments conducted in our laboratory.

RESULTS

NeuroTrace dye labels native NG2-expressing capillary pericytes

Native brain capillary pericytes were isolated using a mechanical and enzymatic isolation method and identified by their “bump-on-a-log” morphology (Fig. 1). This identification was aided by the use of NG2-DsRed-BAC (neural/glial antigen-2-DsRed-bacterial artificial chromosome) transgenic mice expressing the DsRed fluorescent protein under control of the promoter/enhancer for chondroitin sulfate proteoglycan 4 (*Cspg4*; also known as NG2), which is robustly expressed in mural cells (pericytes and SMCs) in the vasculature as well as oligodendrocyte progenitor cells in the CNS. Thus, NG2-positive cells exhibiting the distinct bump-on-a-log morphology—with outward protruding nucleus and elongated processes (Fig. 2 A–D)—were identified as capillary pericytes and readily distinguished from parenchymal arteriole SMCs, which are short, fusiform cells that individually encircle the underlying endothelial layer forming ring-shaped structures (Fig. 2 E and F). Pericyte identification was reinforced by adding NeuroTrace 500/525 to the bath after patch-clamp recordings. This fluorescent Nissl derivative has been reported to specifically target capillary pericytes in the mouse brain in vivo (12). Isolated brain capillary pericytes exhibited intense NeuroTrace labeling in the soma, as well as a punctuate staining pattern along their processes (Fig. 2 A–D). Importantly, NeuroTrace staining co-localized with NG2 expression in capillary pericytes (Fig. 2 A–D) but was absent in NG2-positive arteriolar SMCs (Fig. 2 E and F). Collectively, these observations indicate that the combination of NG2-Red-BAC transgenic mice and post-experimentation staining with NeuroTrace, informed by characteristic morphological features, provides an objective and tractable method for identifying freshly isolated mouse brain capillary pericytes.

Brain capillary pericytes express functional Kir2 channels

Using the conventional whole-cell configuration of the patch-clamp technique, we examined the possible functional expression of strongly inwardly rectifying K⁺ (Kir2) channels in brain capillary pericytes, as has been demonstrated for arterial/arteriolar SMCs. Cells were held at a V_M of −50 mV, dialyzed with a 140 mM K⁺ intracellular solution, and exposed to a high [K⁺] (60 mM) extracellular solution, an experimental paradigm designed to amplify inward Kir currents (Fig. 3 A). Whole-cell currents were recorded in response to 400-ms voltage ramps (−140 to +40 mV) in the absence and presence of Ba²⁺ (100

μM), a pore blocker that is selective for Kir2 channels in the micromolar range (13). Under these experimental conditions, a prominent Ba²⁺-sensitive inward current was observed at voltages negative to E_K (−23 mV), calculated using the Nernst equation (Fig. 3 B and C). At more depolarized potentials (positive to E_K) an outward Ba²⁺-insensitive current was detected (Fig. 3 A and C). Ba²⁺-sensitive currents exhibited the characteristic biophysical profile of the strongly inwardly rectifying Kir2 channel subfamily, similar those observed in endothelial cells and SMCs (13,14). As shown in Fig. 3 C, Ba²⁺ significantly decreased the peak inward current (−140 mV), reducing it by an average of -33.5 ± 12.1 pA/pF, but had no impact on the outward current (Fig. 3 A and C), suggesting that this latter current is mediated by other K⁺ channels. Note, the average current density in 6 mM external K⁺ solutions (-10.3 ± 2.1 pA/pF; $n = 7$ cells) was significantly smaller than that recorded in 60 mM external K⁺ (-44.42 ± 3.5 pA/pF; $n = 15$ cells) at −140 mV. These findings support the idea that brain capillary pericytes express functional Kir2 channels.

Brain capillary pericytes express functional K_V channels

To investigate whether K_V channels mediate the outward current observed at depolarized potentials, we conducted patch-clamp experiments using the conventional whole-cell configuration. Currents were monitored in response to 400-ms voltage steps ranging from −70 to +70 mV in 20-mV increments, starting from a holding potential of −50 mV (Fig. 4 A). Cells were bathed in an extracellular 6 mM KCl solution and dialyzed with a 140 mM pipette solution, resulting in a calculated E_K of approximately −80 mV. Any contribution of potential BK_{Ca} channels to the outward current was prevented by exposing cells to a low extracellular [Ca²⁺] (0.1 mM) and dialyzing them with a solution containing 1 mM Ca²⁺ and 10 mM EGTA (free Ca²⁺ ≈ 20 nM). Upon step depolarizations, outward currents were activated, reaching a peak current at +70 mV, with an end-pulse current density of 48.9 ± 10.4 pA/pF (Fig. 4 A–D and E), demonstrating the functional presence of voltage-sensitive K⁺ channels. To obtain a pharmacological profile of K_V channel currents in brain capillary pericytes, we assessed the inhibitory effect of 4-AP, a K_V1.2/1.5 channel blocker (15,16). 4-AP (1 mM) significantly decreased depolarization-evoked peak outward K⁺ currents (Fig. 4 B–D). After 4-AP application, peak currents and 4-AP-sensitive currents, measured at +70 mV, displayed end-pulse current densities of 32.5 ± 6.5 pA/pF and 16.4 ± 5.2 pA/pF, respectively (Fig. 4 E). We also determined the activation time constants (τ_{act}) by fitting individual voltage-evoked current traces (20-mV increments) to an exponential function. As shown in Fig. 4 F, the rate of activation of the K_V current increased with depolarization, and

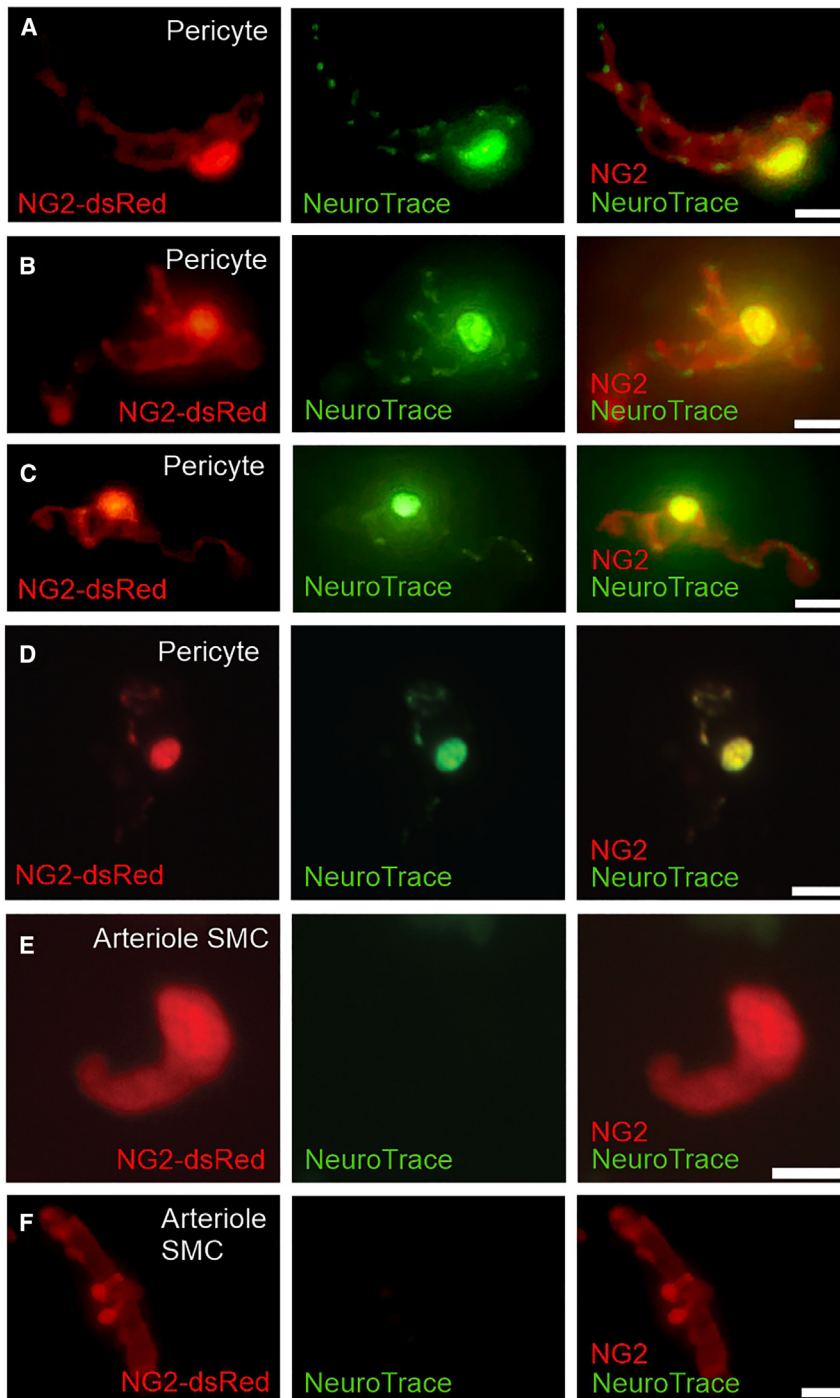


FIGURE 2 NeuroTrace 500/525 dye labels freshly isolated NG2-expressing capillary pericytes. Images of freshly isolated brain capillary pericytes were captured from NG2-DsRed-BAC transgenic mice using a digital camera attached to the microscope (A–C, F) or by z stack imaging using an upright spinning-disk confocal microscope (D and E). (A–D) Robust overlap between the DsRed fluorescence of NG2-expressing capillary pericytes and NeuroTrace 500/525 staining. NeuroTrace labeling appeared bright and intense in the cell soma and along the processes of the pericytes, displaying a punctuate pattern. (E and F) Ring-like parenchymal arteriole NG2-positive SMCs with absent NeuroTrace dye labeling. Each image is representative of images acquired from at least five isolated pericytes from at least three different mice. Scale bars, 10 μm (A–E) and 20 μm (F).

τ_{act} values were comparable in the absence and presence of 4-AP. For example, at +30 mV, the values of τ_{act} were 38.7 ± 6.3 ms and 39.5 ± 6.7 ms, respectively. Finally, the half-maximal activation potential ($V_{0.5}$), obtained by analyzing tail currents, was 18.5 and 20.7 mV in the absence and presence, respectively, of bath-applied 4-AP (Fig. 4 G). These data offer evidence supporting the functional expression of $K_{\text{V}}1$ channels in brain capillary pericytes but do not

rule out the potential presence of other K_{V} channel subtypes, such as $K_{\text{V}}2.1$, $K_{\text{V}}6$, and $K_{\text{V}}9$.

Brain capillary pericytes express BK_{Ca} channels and ryanodine receptors

To test the potential contribution of BK_{Ca} channels to outward currents in native brain capillary pericytes, we first

Sancho et al.

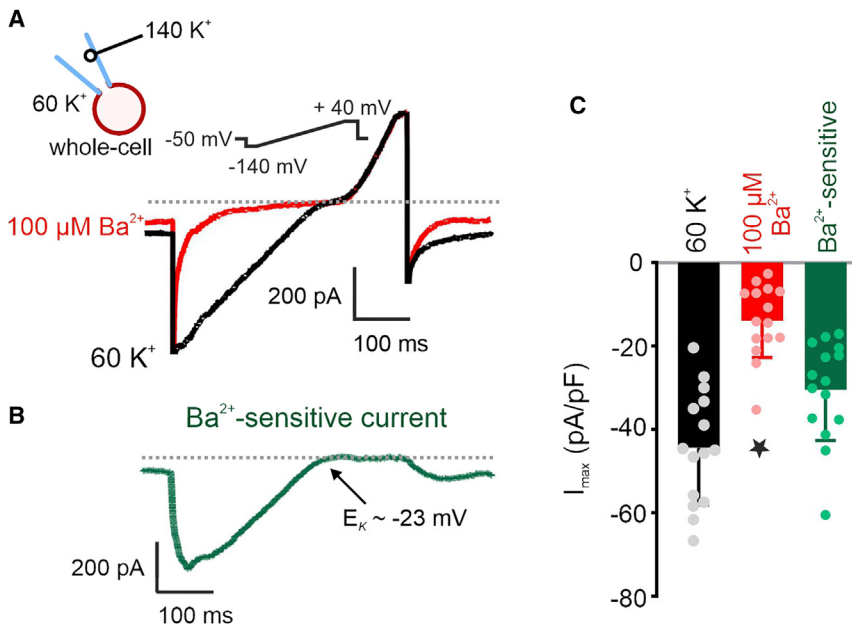


FIGURE 3 Brain capillary pericytes express functional strong inwardly rectifying K⁺ (Kir2) channels. (A) Whole-cell K⁺ currents recorded in isolated pericytes in the absence (*black trace*) and presence (*red trace*) of 100 μM Ba²⁺ showing the large inward component at voltages negative to E_K (−23 mV) and its effective block by Ba²⁺. A modest Ba²⁺-insensitive outward component was present at more depolarized voltages (positive to E_K). Cells were bathed in high [K⁺], and currents were elicited by a 400-ms voltage ramp from −140 to +40 mV (*upper inset*). (B) Ba²⁺-subtracted currents (*green trace*), revealing the classic profile of a strongly rectifying K⁺ current. (C) Summary data comparing peak (−140 mV) inward current density (pA/pF) of control, Ba²⁺ (100 μM), and Ba²⁺-sensitive currents (*n* = 15 cells from seven mice). Dotted line represents zero current level. Values are presented as means ± SD (**p* < 0.05; paired *t*-test). External and internal [K⁺] were 60 and 140 mM, respectively.

employed the conventional whole-cell configuration of the patch-clamp technique. Pericytes were bathed in an extracellular 6 mM KCl solution and dialyzed with a 140 mM intracellular solution (E_K ≈ −80 mV) containing 300 nM free Ca²⁺ to stimulate BK_{Ca} channels. Under these experimental conditions, a large outward K⁺ current was recorded in response to 400-ms voltage steps ranging from −70 to +70 mV (in 20-mV increments) from a holding potential of −50 mV (Fig. 5 A). The functional expression of BK_{Ca} channels was tested by exposing the cells to paxilline (1 μM), a specific blocker of BK_{Ca} channels (17,18). Addition of paxilline to the bath reduced the density of depolarization-activated steady-state currents by ~72%. At +70 mV, the measured end-pulse current density was reduced from 57.9 ± 23.3 pA/pF to 16.2 ± 5.9 pA/pF (Fig. 5 A and B). A similar, albeit slightly more modest, inhibitory effect (~40% reduction) on outward currents was obtained by incubating cells with iberiotoxin (IbTx; 100 nM) (Fig. 5 C), another highly selective blocker of BK_{Ca} channels (18,19). The resulting IbTx-sensitive end-pulse current density measured at +70 mV was 23.9 ± 10.6 pA/pF (Fig. 5 D). Notably, every cell tested displayed these currents, supporting the functional expression of BK_{Ca} channels in all brain capillary pericytes.

To provide further evidence for the functional expression of BK_{Ca} channels in a cellular context, we next investigated the occurrence of STOCs, macroscopic currents mediated by BK_{Ca} channels in response to stimulation by Ca²⁺-release events (Ca²⁺ sparks) from the sarcoplasmic reticulum via ryanodine receptors (RyRs) (20). To this end, we patch clamped native pericytes in the amphotericin B-perforated configuration and monitored STOCs at a holding voltage of −20 mV. In the absence of any specific BK_{Ca}

blockers, STOCs were detected with a frequency of 2.2 ± 0.4 Hz and an amplitude of 19.5 ± 4.1 pA (Fig. 5 E). We next examined the effects of the BK_{Ca} blockers, paxilline and IbTx, on STOC activity. Bath application of paxilline (1 μM) produced inhibitory effects within 30 s, leading to a significant decrease in both the frequency (0.2 ± 0.2 Hz) and amplitude (16.1 ± 6.8 pA) of STOCs. Notably, paxilline completely abolished STOCs after 1 min of exposure, confirming its rapid and strong inhibitory effect (Fig. 5 E). After 1 min of incubation, IbTx (100 nM) markedly reduced the frequency of STOCs (0.3 ± 0.2 Hz) compared with that observed in its absence (2.2 ± 0.4 Hz). STOCs were eliminated 2 min after IbTx application (Fig. 5 F). We further explored the role of RyR-mediated Ca²⁺ sparks in driving STOCs, testing the effects of the selective RyR blocker, ryanodine, on the occurrence and characteristics of STOCs. Ryanodine (20 μM) progressively reduced the frequency of STOCs from 2.2 ± 0.6 Hz to 0.6 ± 0.3 Hz; it also decreased the amplitude of STOCs from 18.8 ± 4.5 pA to 15.1 ± 1.9 pA (Fig. S1). Notably, a fraction (~20%) of pericytes tested showed no STOC activity. Whether this reflects physiologically meaningful heterogeneity of ion channel surface expression or among pericytes, such as patchy or capillary region-specific BK_{Ca} expression, or experimental issues remains to be tested. Collectively, these observations reinforce the conclusion that BK_{Ca} channels are expressed in brain capillary pericytes and imply the functional expression of RyRs in the sarcoplasmic reticulum membrane of these cells and their involvement in Ca²⁺ spark-driven BK_{Ca} currents.

The single-channel properties of BK_{Ca} channels were further explored in native brain capillary pericytes using the cell-attached mode of the patch-clamp technique. These

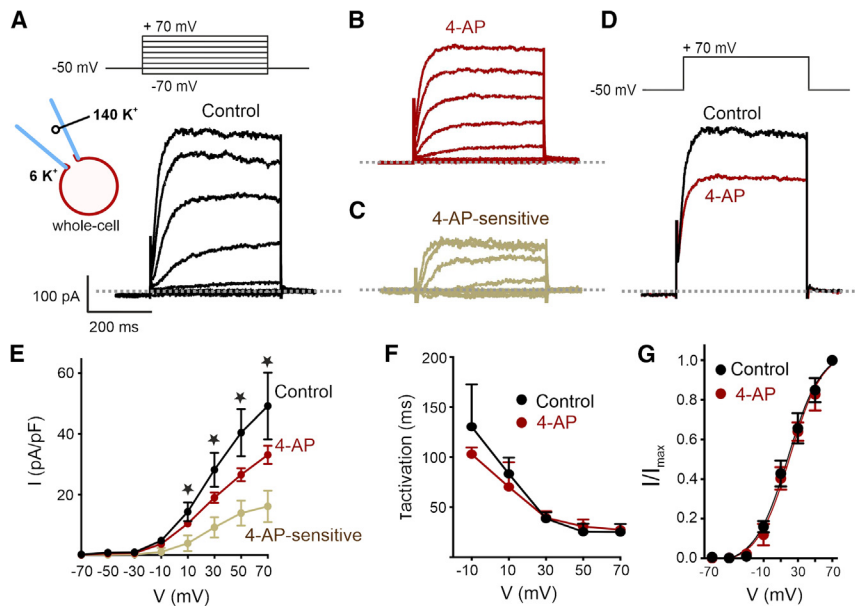


FIGURE 4 Functional voltage-gated K^+ (K_V) channels are present in brain capillary pericytes. Original traces of whole-cell K^+ currents recorded from an isolated brain pericyte before (A; *black trace*) and after (B; *red trace*) treatment with 4-AP (1 mM). Currents were elicited by voltage steps from -70 to $+70$ mV from a holding potential of -50 mV. (C) 4-AP-sensitive currents (*dark yellow trace*) obtained after subtracting the original recordings plotted in (A) and (B) indicating the presence of functional K_V channels in brain pericytes. (D) Original traces of whole-cell currents elicited by a voltage step to $+70$ mV from holding potential of -50 mV in the absence (*black trace*) and presence (*red trace*) of the $K_V1.2/1.5$ inhibitor 4-AP (1 mM). (E) Whole-cell current-voltage relationship, measured at peak outward current at each test potential corresponding to control, 4-AP-treated, and 4-AP-sensitive currents ($n = 8$ cells from three mice). (F) Activation time constants (τ activation) obtained from an exponential fit of individual voltage-evoked (20-mV pulses) current recordings obtained before (*black trace*) and after (*red trace*) application of 1 mM 4-AP ($n = 8$ cells from three mice). (G) Steady-state activation properties of K_V currents ($n = 8$ cells from three mice). The half-maximal activation voltage ($V_{0.5}$) was determined from a fit of the data to the Boltzmann equation. Dotted line represents zero current level. Values are presented as means \pm SD (* $p < 0.05$; Wilcoxon matched-pairs signed-rank test). External and internal $[K^+]$ were 6 and 140 mM, respectively.

experiments were conducted in symmetrical 140/140 mM KCl extra and intracellular solutions, yielding a reversal potential of 0 mV. After achieving a $G\Omega$ seal, patches were held at voltages ranging from 0 to $+100$ mV (applied voltage, 0 to -100 mV) in 20-mV increments (Fig. 6 A). At -100 mV, the single-channel unitary current was 4.5 ± 0.2 pA at $+20$ mV and increased to 22.9 ± 0.3 pA at $+100$ mV (Fig. 6 A and B). The single-channel conductance was 227.6 pS (Fig. 6 B), strongly indicative of BK_{Ca} channels. An analysis of the dependence of the channel activity on the applied potential showed that the average open probability (NP_o) of the channel, reflecting the number of channels in the patch (N) and their open probability (P_o), increased with membrane depolarization, a fundamental property of BK_{Ca} channels (21). For example, NP_o was 0.008 ± 0.1 at $+20$ mV and increased to 0.389 ± 0.3 at $+100$ mV ($n = 12$ cells from five mice). Overall, these findings confirm the expression of BK_{Ca} channels in native brain capillary pericytes and provide valuable insights into their electrophysiological features.

DISCUSSION

The complex network of interconnected surface arteries and branching penetrating arterioles of the brain feed a dense web of capillaries that bring cECs into close proximity (~ 10 – $20 \mu m$) to all neurons in the parenchyma (2). We previously demonstrated that brain capillaries function as efficient sensors of neuronally released K^+ through the activation of endothelial Kir2.1 channels, which initiates a retrograde, electrical (hyperpolarizing) signal that rapidly propagates upstream to cause arteriole dilation and localized

increases in CBF to the active neural site (14). The V_M of vascular cells is crucial in this process, as it serves as the physiological connection that converts electrical signals into vascular responses. Within this framework, we recently established that both capillary cellular constituents—cECs and pericytes—are molecularly equipped to respond to the brain-derived vasoactive mediator, adenosine, through K_{ATP} channels, which exert a robust influence on capillary V_M and the regulation of brain blood flow (10). Here, we explored the repertoire of K^+ channel currents involved in setting V_M in freshly isolated brain capillary pericytes—reliably identified by applying morphological criteria and staining with NeuroTrace (a fluorescent Nissl dye) in NG2-DsRed transgenic mice—using different configurations of the patch-clamp technique. The unique electrophysiological signature of Kir2 channels—inward rectification at V_M negative to E_K and activation by external K^+ —make these channels ideal candidates for setting the resting V_M of vascular SMCs (6,7,13). Consistent with this, we demonstrated the functional expression of an inward current mediated by Kir2 channels, identified based on their unique biophysical signature and sensitivity to micromolar concentrations of Ba^{2+} . Based on sensitivity to specific blockers, kinetics, and characteristic electrical features, we further revealed the presence of two voltage-dependent outward currents mediated by K_V1 and BK_{Ca} channels in brain capillary pericytes. Collectively, our data provide multiple lines of evidence supporting the functional expression of Kir2, K_V1 , and BK_{Ca} channels with potentially significant roles in the regulation of CBF in brain capillary pericytes.

The Kir2 currents from freshly isolated brain capillary pericytes possessed electrical properties comparable to

Sancho et al.

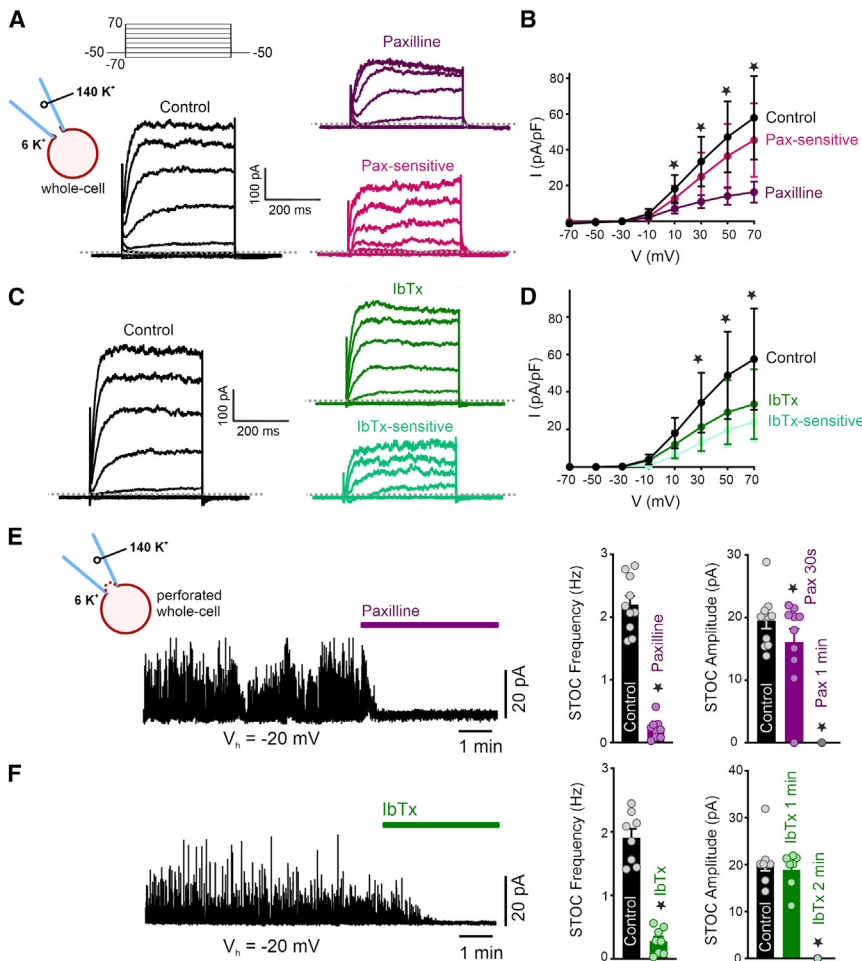


FIGURE 5 Brain capillary pericytes possess large-conductance Ca^{2+} -activated K^+ (BK_{Ca}) channels. (A) Representative traces of whole-cell K^+ currents recorded from an isolated brain pericyte before (black trace) and after (purple trace) application of $1 \mu\text{M}$ paxilline. Dark pink trace indicates paxilline-sensitive currents obtained by subtracting currents before and after paxilline treatment. Currents were elicited by voltage steps from -70 to $+70$ mV from a holding potential of -50 mV. (B) Summary data showing peak outward current at each holding potential corresponding to control, paxilline-treated, and paxilline-sensitive currents ($n = 9$ cells from three mice). (C) Original traces of whole-cell currents recorded from a native brain pericyte before (black trace) and after (dark green trace) application of 100 nM iberiotoxin (IbTx). Light green trace indicates IbTx-sensitive currents obtained by subtracting currents before and after IbTx application. (D) Whole-cell current-voltage relationship, measured at peak outward current at each voltage, corresponding to control, IbTx-treated, and IbTx-sensitive currents ($n = 6$ cells from three mice). (E) Perforated patch-clamp traces (left) and summary data showing STOCs frequency (middle) and amplitude (right) in the absence and the presence of paxilline ($1 \mu\text{M}$) ($n = 10$ cells from four mice). Currents were recorded at a holding potential of -20 mV. (F) Original traces (left) and averaged data for STOC frequency (middle) and amplitude (right) before and after treatment with IbTx (100 nM) ($n = 8$ cells from three mice). Currents were recorded at a holding potential of -20 mV. Dotted line represents zero current level. Values are presented as means \pm SD ($*p < 0.05$; Wilcoxon matched-pairs signed-rank test). External and internal $[\text{K}^+]$ were 6 and 140 mM, respectively.

those observed in their arterial/arteriolar SMC counterparts, which specifically express the Kir2.1 isoform (14,22–24), and in fresh and cultured retinal pericytes (25,26). Single-cell RNA sequencing data indicating robust expression of the gene encoding the Kir2.2 subunit (*Kcnj12*) in pericytes isolated from the mouse brain (9) suggest that the Kir2 currents identified here could be mediated by the Kir2.2 isoform, a conclusion echoed by a recent report (27). Nevertheless, a definitive conclusion will require a more precise investigation into the Kir2 subunits expressed in pericytes.

Voltage-dependent K^+ (K_{V}) channels, which are prominently expressed in rodent brain arterial/arteriolar SMCs, open in response to membrane depolarization, facilitating the efflux of K^+ ions and consequently counteracting further depolarizing influences (i.e., intraluminal pressure or vasoconstrictor agents), thus acting as a brake on vasoconstriction (6,28,29). Of the 12 different subtypes ($\text{K}_{\text{V}}1$ – 12) in the $\text{K}_{\text{V}}1$ family, 4-AP-sensitive (30) $\text{K}_{\text{V}}1.2$ and $\text{K}_{\text{V}}1.5$ channels are the primary subtypes expressed in brain parenchymal arteriolar SMCs (28,29). The 4-AP-sensitive, voltage-dependent outward current identified in capillary

pericytes exhibited fast activation kinetics in response to depolarized potentials, with τ_{act} values in the range of tens of milliseconds. However, compared with $\text{K}_{\text{V}}1$ currents recorded in mouse arteriolar SMCs (28,29), the $V_{0.5}$ values obtained in brain pericytes were positively shifted ($+18.5$ vs. $+6$ mV), indicating potential differences in $\text{K}_{\text{V}}1$ channel subunit stoichiometry compared with those in brain arteriolar SMCs (28). Our study represents an initial step in delineating which K_{V} channels are functionally expressed in CNS pericytes. Understanding the molecular mechanisms and potential roles played by these channels in the dynamic landscape of CNS pericytes will ultimately require analyses that delve more deeply into the expression of specific subfamily members, including $\text{K}_{\text{V}}1.2/1.5$ and $\text{K}_{\text{V}}2.1$, alone or through formation of heteromultimers with $\text{K}_{\text{V}}6$ or $\text{K}_{\text{V}}9$ subunits (30).

Our whole-cell and single-channel recordings also demonstrated the presence of a third current in brain capillary pericytes with properties similar to those of SMC BK_{Ca} channels, including high K^+ selectivity, a large single-channel conductance (~ 228 pS), and an open probability that is both voltage and Ca^{2+} dependent (21,31–33). The

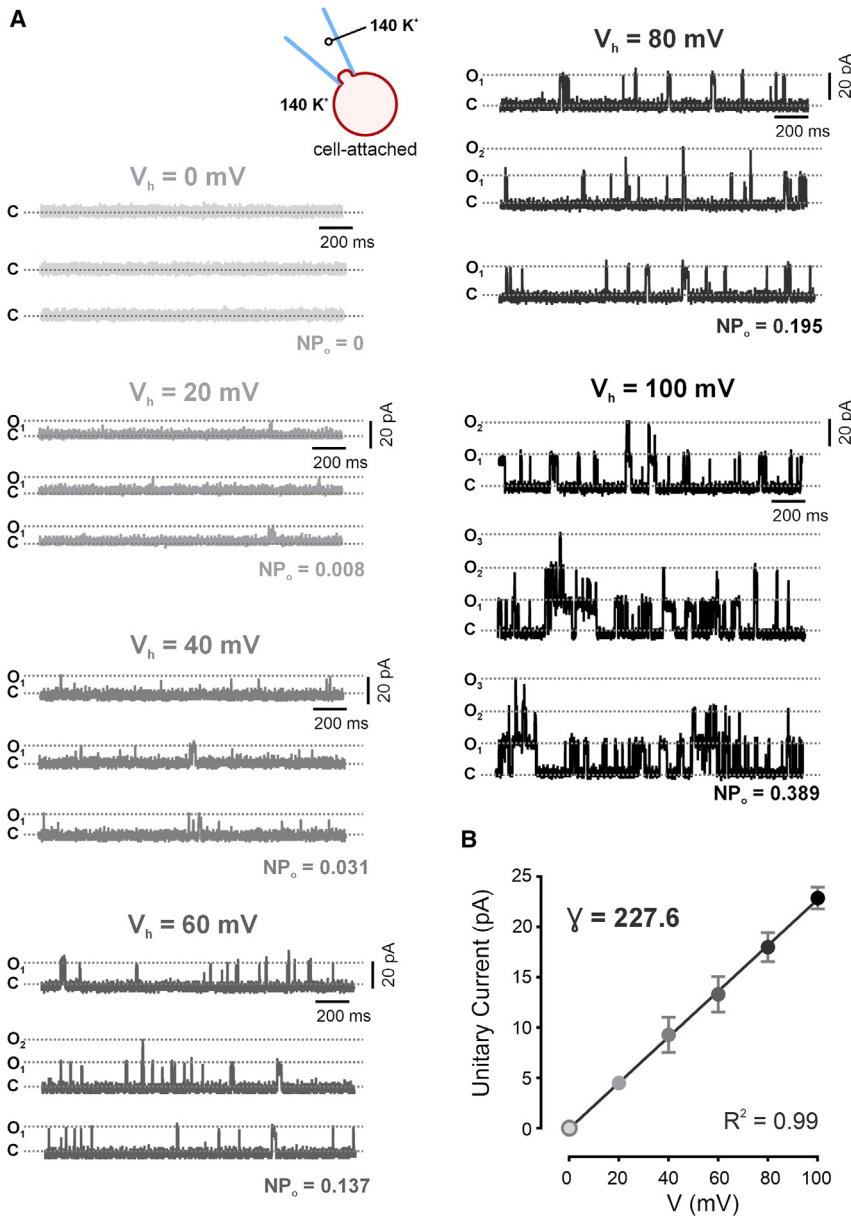


FIGURE 6 Single-channel properties of large-conductance Ca^{2+} -activated K^+ (BK_{Ca}) channels expressed in brain capillary pericytes. (A) Representative single-channel recordings from brain pericytes, obtained using the cell-attached configuration and symmetrical 140/140 mM bath (extra-) and pipette (intracellular) solutions. Single-channel events were recorded from a range of applied potentials from 0 to +100 mV (in 20-mV increments). The averaged open probabilities (NP_o) are displayed for each holding potential. C, closed state; O_1 , O_2 , and O_3 , open states. (B) Plot of unitary current-voltage relationship based on averaged unitary currents measured at 0 mV ($n = 8$ cells from five mice), +20 mV ($n = 8$ cells from five mice), +40 mV ($n = 9$ cells from five mice), +60 mV ($n = 9$ cells from five mice), +80 mV ($n = 9$ cells from five mice), and +100 mV ($n = 12$ from five mice). The single-channel conductance, obtained from the slope of the linear fit, was determined to be 227.6 pS. Values are presented as means \pm SD. Dotted line in (B) represents zero unitary current level.

sensitivity of this current to the specific blockers, paxilline and iberiotoxin (34), and their generation of STOCs in response to RyR-mediated Ca^{2+} sparks further strengthens this identification. These findings are consistent with prior research conducted in cultured retinal pericytes (26,35) and align with recent work demonstrating the involvement of RyR-mediated Ca^{2+} release from the sarcoplasmic reticulum in the generation of spontaneous Ca^{2+} transients in brain capillary pericytes (36). However, they are seemingly at odds with our previous imaging results obtained using an en face retinal microvasculature preparation. In this latter study, we reported no contribution of RyRs to pericyte-localized Ca^{2+} events in response to application of caffeine, which induces acute release of Ca^{2+} from intracellular

stores. Although routinely used experimentally as an indicator of RyR function, this approach lacks the nuance of the electrophysiological approach used in the current study, especially when applied to an intact system. It is also worth noting that the Ca^{2+} events imaged in our previous study were specific to pericytes in the arteriole-capillary transition region, whereas the results reported here are for pericytes generally, without regard to their location in the arteriole proximate-to-distal continuum. In SMCs, BK_{Ca} channels play a key role in opposing myogenic responses, serving to maintain vessels in a partially constricted state under physiological conditions (34). In pericytes, with their high input resistance and unitary conductance (~ 200 pS), the opening of even a few BK_{Ca} channels could exert a

Sancho et al.

significant hyperpolarizing impact on V_M . In a physiological setting, activation of pericyte BK_{Ca} channels by depolarization or elevated intracellular Ca^{2+} would lead to membrane hyperpolarization, acting as a brake to counter further depolarization.

Understanding the functional ion channel repertoire in brain capillary cells is essential for unraveling their biophysical features and specific contributions to capillary hemodynamics. In this context, recent work from our lab has begun to define the electrophysiological fingerprint of brain cECs (10,14,37,38), yet direct measurements of key ion channel currents in native brain pericytes have remained limited (8,10). This is important given the known significant influence of pericytes on basal capillary diameter and fine control of CBF (4,8,39). CNS capillary pericytes are electrically excitable cells capable of responding to diverse neural-mediated vasoactive substances (10,40). Using our *ex vivo* pressurized retina preparation and microelectrodes, we previously found that capillary pericytes display a fairly depolarized resting V_M (-30 to -40 mV) relative to that of arteriolar SMCs (-60 mV) under physiological pressure conditions, consistent with a relatively low K^+ permeability (8,10). Additionally, direct patch-clamp measurements revealed a unique current-voltage relationship, distinct from their vascular counterparts, including cECs, arteriolar ECs, and SMCs (10,14,22). This distinctive profile is marked by a pronounced, nonlinear inward K^+ current at hyperpolarized potentials relative to E_K (approximately -23 mV) in cells exposed to 60 mM extracellular $[K^+]$ and a more modest outward current at depolarized voltages (10). These findings imply the involvement of different K^+ ion channels in governing pericyte V_M and capillary perfusion.

The substantial difference in V_M observed between CNS pericytes (~ 40 mV) and SMCs (~ 60 mV) under low-pressure conditions is intriguing and offers insights into the electrophysiological characteristics of these cell types. Placing this in a physiological context, it is possible that decreased Ca^{2+} spark and BK_{Ca} channel activity, and thus relatively diminished outward currents, contribute to the characteristic depolarized state of this particular cell type. In fact, the BK_{Ca} current density in capillary brain pericytes is substantially smaller (about sixfold) than that in cerebral arterial SMCs. Alternatively, the depolarized V_M in CNS pericytes could be attributable to elevated inward currents resulting from the increased activity of as-yet-undefined ion channel types. Our understanding of the electrophysiological properties of brain capillary pericytes is currently in its early stages, and additional research is essential to uncover the underlying mechanisms of these disparities in V_M and ion channel activity and delineate their functional consequences.

One notable limitation of the present study is the observed low success rate encountered in patching pericytes. Despite significant effort and the establishment of

an isolation protocol yielding viable pericytes, the patching success rate, including drug application, remains modest. Additionally, pericytes exhibit differences in morphology and functional characteristics depending on their anatomical location within the brain microvasculature (specifically, their position along the arteriole proximate-to-distal continuum). Thus, another challenge in conducting patch-clamp analyses on capillary pericytes isolated from brain tissue is the inability to discern which specific pericyte subtype is being recorded. This limitation raises several intriguing questions worthy of further investigation. How does the repertoire of ion channels, and thus biophysical properties of the cell, vary according to anatomical position of the pericyte? How does the varying biophysical profile of pericytes reflect their functional roles? And how does the heterogeneous mixture of pericyte subtypes in brain tissue microvasculature isolates affect the interpretation of our findings? An intact, pressurized retina preparation that we have recently developed, which allows us to precisely impale a cell of interest and measure its V_M (8), may be useful in addressing questions related to differences in the biophysical properties of pericytes at different points in the microvasculature. However, the interpretation of the resulting findings is complex due to the likely electrical communication between pericytes and cECs. Pericyte subtype-specific Cre drivers should aid interpretation of specific ion channel subtype differences. Combining and optimizing these distinct electrophysiological approaches could enable us to develop a more comprehensive understanding of the electrical properties and functional roles of subtypes of CNS pericytes.

Collectively, our results provide multiple lines of evidence supporting the expression of functional Kir2, K_V1 , and BK_{Ca} channels in brain capillary pericytes. This work represents an initial step in delineating the functional expression of these three distinct channel types and suggests their possible contribution in orchestrating the V_M of brain capillary pericytes, with profound implications for capillary hemodynamics and the control of CBF. Although this study demonstrates that pericytes are equipped with essential molecular components, the precise role of these specific K^+ channel families in a physiological context is yet to be fully defined. More specific pharmacological strategies and complementary *in situ* membrane potential recordings may help decipher the specific expression of particular subfamily members, particularly in K_V channels. The physiological and pathological relevance of the distinct signaling pathways involving pericyte K^+ channels and CBF control represents an exciting area for future research.

SUPPORTING MATERIAL

Supporting Material can be found online at <https://doi.org/10.1016/j.bpj.2024.03.004>.

AUTHOR CONTRIBUTIONS

M.S. designed the study, performed research, and analyzed data. N.R.K. assisted with microphotographs acquisition. O.F.H. provided analysis assistance. M.S. and M.T.N. wrote the paper. D.H.-E. organized the presentation and edited the manuscript. M.T.N. provided conceptual context and edited the manuscript.

ACKNOWLEDGMENTS

We thank T. Wellman and D. Enders for technical assistance. Research reported in this publication was supported by the National Heart, Lung, and Blood Institute of the National Institutes of Health (F32HL152576 to N.R.K.; R01HL169681 to O.F.H.) and the American Heart Association (Career Development Awards 23CDA1050558 to N.R.K.; 20CDA35310097 to O.F.H.). Support was also provided by the Totman Medical Research Trust (to M.T.N. and O.F.H.); the Bloomfield Professorship in Cardiovascular Research (to O.F.H.); the Larner College of Medicine, University of Vermont, and the Cardiovascular Research Institute of Vermont (to O.F.H.); the European Union Horizon 2020 Research and Innovation Programme (grant agreement 666881, SVDs@target, to M.T.N.); as well as grants from the National Institute of Neurological Disorders and Stroke (NINDS) and National Institute on Aging (NIA) (R01-NS-110656 and 1RF1NS128963 to M.T.N.; R21AG082193 to O.F.H.), the National Institute of General Medical Sciences (NIGMS) (P20-GM-135007 to M.T.N.; P20GM135007 to O.F.H.), and the National Heart, Lung, and Blood Institute (NHLBI) of the NIH (R35-HL-140027 to M.T.N.).

DECLARATION OF INTERESTS

The authors declare no competing interests.

REFERENCES

- Gould, I. G., P. Tsai, ..., A. Linninger. 2017. The capillary bed offers the largest hemodynamic resistance to the cortical blood supply. *J. Cerebr. Blood Flow Metabol.* 37:52–68.
- Attwell, D., A. M. Buchan, ..., E. A. Newman. 2010. Glial and neuronal control of brain blood flow. *Nature (London, U. K.)* 468:232–243.
- Knot, H. J., and M. T. Nelson. 1998. Regulation of arterial diameter and wall [Ca²⁺] in cerebral arteries of rat by membrane potential and intravascular pressure. *J. Physiol.* 508:199–209.
- Gonzales, A. L., N. R. Klug, ..., M. T. Nelson. 2020. Contractile pericytes determine the direction of blood flow at capillary junctions. *Proc. Natl. Acad. Sci. USA.* 117:27022–27033.
- Nystoriak, M. A., K. P. O'Connor, ..., G. C. Wellman. 2011. Fundamental increase in pressure-dependent constriction of brain parenchymal arterioles from subarachnoid hemorrhage model rats due to membrane depolarization. *Am. J. Physiol. Heart Circ. Physiol.* 300:H803–H812.
- Nelson, M. T., and J. M. Quayle. 1995. Physiological roles and properties of potassium channels in arterial smooth muscle. *Am. J. Physiol.* 268 (4 Pt 1):C799–C822.
- Nelson, M. T., J. B. Patlak, ..., N. B. Standen. 1990. Calcium channels, potassium channels, and voltage dependence of arterial smooth muscle tone. *Am. J. Physiol.* 259:C3–C18.
- Klug, N. R., M. Sancho, ..., M. T. Nelson. 2023. Intraluminal pressure elevates intracellular calcium and contracts CNS pericytes: Role of voltage-dependent calcium channels. *Proc. Natl. Acad. Sci. USA.* 120, e2216421120.
- Vanlandewijck, M., L. He, ..., C. Betsholtz. 2018. A molecular atlas of cell types and zonation in the brain vasculature. *Nature.* 554:475–480.
- Sancho, M., N. R. Klug, ..., M. T. Nelson. 2022. Adenosine signaling activates ATP-sensitive K⁺ channels in endothelial cells and pericytes in CNS capillaries. *Sci. Signal.* 15:eab15405.
- Vanlandewijck, M., M. Vanlandewijck, ..., C. Betsholtz. 2018. Primary isolation of vascular cells from murine brain for single cell sequencing. *Protoc. Exch.* 1–11.
- Damisah, E. C., R. A. Hill, ..., J. Grutzendler. 2017. A FluoroNissl dye identifies pericytes as distinct vascular mural cells during in vivo brain imaging. *Nat. Neurosci.* 20:1023–1032.
- Quayle, J. M., J. G. McCarron, ..., M. T. Nelson. 1993. Inward rectifier K⁺ currents in smooth muscle cells from rat resistance-sized cerebral arteries. *Am. J. Physiol.* 265 (5 Pt 1):C1363–C1370.
- Longden, T. A., F. Dabertrand, ..., M. T. Nelson. 2017. Capillary K⁺-sensing initiates retrograde hyperpolarization to increase local cerebral blood flow. *Nat. Neurosci.* 20:717–726.
- Gutman, G. A., K. G. Chandy, ..., X. Wang. 2005. International Union of Pharmacology. LIII. Nomenclature and molecular relationships of voltage-gated potassium channels. *Pharmacol. Rev.* 57:473–508.
- Robertson, B. E., and M. T. Nelson. 1994. Aminopyridine inhibition and voltage dependence of K⁺ currents in smooth muscle cells from cerebral arteries. *Am. J. Physiol.* 267:C1589–C1597.
- Knaus, H.-G., O. B. McManus, ..., A. B. Smith, 3rd. 1994. Tremorgenic Indole Alkaloids Potently Inhibit Smooth Muscle High-Conductance Calcium-Activated Potassium Channels. *Biochemistry.* 33:5819–5828.
- Latorre, R., K. Castillo, ..., O. Alvarez. 2017. Molecular Determinants of BK Channel Functional Diversity and Functioning. *Physiol. Rev.* 97:39–87.
- Candia, S., M. L. Garcia, and R. Latorre. 1992. Mode of action of ibertoxin, a potent blocker of the large conductance Ca(2+)-activated K+ channel. *Biophys. J.* 63:583–590.
- Nelson, M. T., H. Cheng, ..., W. J. Lederer. 1995. Relaxation of arterial smooth muscle by calcium sparks. *Science.* 270:633–637.
- Cui, J., D. H. Cox, and R. W. Aldrich. 1997. Intrinsic Voltage Dependence and Ca²⁺ Regulation of mslo Large Conductance Ca-activated K⁺ Channels. *J. Gen. Physiol.* 109:647–673.
- Sonkusare, S. K., T. Dalsgaard, ..., M. T. Nelson. 2016. Inward rectifier potassium (Kir2.1) channels as end-stage boosters of endothelium-dependent vasodilators. *J. Physiol.* 594:3271–3285.
- Quayle, J. M., M. T. Nelson, and N. B. Standen. 1997. ATP-sensitive and inwardly rectifying potassium channels in smooth muscle. *Physiol. Rev.* 77:1165–1232.
- Bradley, K. K., J. H. Jaggar, ..., B. Horowitz. 1999. *ir 2.1* encodes the inward rectifier potassium channel in rat arterial smooth muscle cells. *J. Physiol.* 515:639–651.
- Matsushita, K., and D. G. Puro. 2006. Topographical heterogeneity of KIR currents in pericyte-containing microvessels of the rat retina: Effect of diabetes. *J. Physiol.* 573:483–495.
- Quignard, J. F., E. A. Harley, ..., M. Félétou. 2003. K⁺ channels in cultured bovine retinal pericytes: Effects of β -adrenergic stimulation. *J. Cardiovasc. Pharmacol.* 42:379–388.
- Glück, C., K. D. Ferrari, ..., B. Weber. 2021. Distinct signatures of calcium activity in brain mural cells. *Elife.* 10, e70591.
- Dabertrand, F., C. Krøigaard, ..., M. T. Nelson. 2015. Potassium channelopathy-like defect underlies early-stage cerebrovascular dysfunction in a genetic model of small vessel disease. *Proc. Natl. Acad. Sci. USA.* 112.
- Straub, S. V., H. Girouard, ..., M. T. Nelson. 2009. Regulation of intracerebral arteriolar tone by K(v) channels: effects of glucose and PKC. *Am. J. Physiol. Cell Physiol.* 297:C788–C796.
- Moreno-Domínguez, A., P. Ciudad, ..., M. T. Pérez-García. 2009. De novo expression of Kv6.3 contributes to changes in vascular smooth muscle cell excitability in a hypertensive mice strain. *J. Physiol.* 587:625–640.

Sancho et al.

31. Brenner, R., G. J. Pérez, ..., R. W. Aldrich. 2000. Vasoregulation by the $\beta 1$ subunit of the calcium-activated potassium channel. *Nature*. 407:870–876.
32. Horrigan, F. T., and R. W. Aldrich. 2002. Coupling between Voltage Sensor Activation, Ca^{2+} Binding and Channel Opening in Large Conductance (BK) Potassium Channels. *J. Gen. Physiol.* 120:267–305.
33. Cox, D. H., J. Cui, and R. W. Aldrich. 1997. Allosteric Gating of a Large Conductance Ca-activated K^{+} Channel. *J. Gen. Physiol.* 110:257–281.
34. Brayden, J. E., and M. T. Nelson. 1992. Regulation of arterial tone by activation of calcium-dependent potassium channels. *Science*. 256:532–535.
35. Berweck, S., A. Lepple-Wienhues, ..., M. Wiederholt. 1994. Large conductance calcium-activated potassium channels in cultured retinal pericytes under normal and high-glucose conditions. *Pflügers Archiv*. 427:9–16.
36. Phillips, B., J. Clark, ..., R. L. Rungta. 2023. Orai, RyR, and IP3R channels cooperatively regulate calcium signaling in brain mid-capillary pericytes. *Commun. Biol.* 6:493.
37. Harraz, O. F., T. A. Longden, ..., M. T. Nelson. 2018. PIP 2 depletion promotes TRPV4 channel activity in mouse brain capillary endothelial cells. *Elife*. 7, e38689.
38. Harraz, O. F., N. R. Klug, ..., M. T. Nelson. 2022. Piezo1 Is a Mechanosensor Channel in Central Nervous System Capillaries. *Circ. Res.* 130:1531–1546.
39. Sweeney, M. D., S. Ayyadurai, and B. V. Zlokovic. 2016. Pericytes of the neurovascular unit: key functions and signaling pathways. *Nat. Neurosci.* 19:771–783.
40. Matsushita, K., M. Fukumoto, ..., D. G. Puro. 2010. Diabetes-Induced Inhibition of Voltage-Dependent Calcium Channels in the Retinal Microvasculature: Role of Spermine. *Invest. Ophthalmol. Vis. Sci.* 51:5979–5990.